HHS Public Access

Author manuscript

J Psychopharmacol. Author manuscript; available in PMC 2021 November 09.

Published in final edited form as:

J Psychopharmacol. 2020 December ; 34(12): 1393–1407. doi:10.1177/0269881120944160.

Genetic deletion of *Rgs12* in mice affects serotonin transporter expression and function *in vivo* and *ex vivo*

Allison N. White[1], **Joshua D. Gross**[1], **Shane W. Kaski**[1,2], **Kristen R. Trexler**[1,3], **Kim A. Wix**[1], **William C. Wetsel**[4,5], **Steven G. Kinsey**[1,3], **David P. Siderovski**[1], **Vincent Setola**[1,2,*]

[1]Department of Neuroscience, West Virginia University, Morgantown WV 26506 USA

[2]Department of Behavioral Medicine & Psychiatry, West Virginia University, Morgantown WV 26506 USA

[3]Department of Psychology, West Virginia University, Morgantown WV 26506 USA

[4]Mouse Behavioral and Neuroendocrine Analysis Core Facility, Department of Psychiatry and Behavioral Sciences, Duke University Medical Center, Durham NC 27710 USA

[5]Departments of Cell Biology and Neurobiology, Duke University Medical Center, Durham NC 27710 USA

Abstract

Background: Regulator of G protein Signaling (RGS) proteins inhibit G protein-coupled receptor (GPCR) signaling, including the signals that arise from neurotransmitter release. We have shown that RGS12 loss diminishes locomotor responses of C57BL/6J mice to dopamine transporter (DAT)-targeting psychostimulants. This diminution resulted from a brain region-specific upregulation of DAT expression and function in RGS12-null mice. This effect on DAT prompted us to investigate whether the serotonin transporter (SERT) exhibits similar alterations upon RGS12 loss in C57BL/6J mice.

Aims: Does RGS12 loss affect 1) hyperlocomotion to the preferentially SERT-targeting psychostimulant 3,4-methylenedioxymethamphetamine (MDMA), 2) SERT expression and function in relevant brain regions, and/or 3) serotonergically modulated behaviors?

Methods: Open-field and spontaneous home-cage locomotor activities were quantified. 5-HT, 5-HIAA, and SERT levels in brain-region homogenates, as well as SERT expression and function in brain-region tissue preparations, were measured using appropriate biochemical assays. Serotonergically modulated behaviors were assessed using forced swim and tail suspension paradigms, elevated plus and elevated zero maze tests, and social interaction assays.

Results: RGS12-null mice displayed no hyperlocomotion to 10 mg/kg MDMA. There were brain region-specific alterations in SERT expression and function associated with RGS12 loss.

[*]**Corresponding author:** Dr. Vincent Setola, Department of Neuroscience, West Virginia University School of Medicine, 108 Biomedical Road, WVU Health Sciences Center, Morgantown, WV 26506; vssetola@hsc.wvu.edu.
New addresses: Dr. Joshua Gross, Departments of Cell Biology and Neurobiology, Duke University Medical Center, Durham NC 27710 USA; Dr. Steven Kinsey, Center for Advancement in Managing Pain, University of Connecticut, Storrs, CT 06269 USA; Dr. David Siderovski, Department of Pharmacology & Neuroscience, University of North Texas Health Science Center, Fort Worth, TX 76107 USA.

Drug-naïve RGS12-null mice displayed increases in both anxiety-like and anti-depressive-like behaviors.

Conclusion: RGS12 is a critical modulator of serotonergic neurotransmission and serotonergically modulated behavior in mice; lack of hyperlocomotion to low dose MDMA in RGS12-null mice is related to an alteration of steady-state SERT expression and 5-HT uptake.

Keywords

MDMA; Regulators of G protein Signaling; RGS12; serotonergically modulated behaviors; serotonin transporter

Introduction

Serotonin (5-HT), widely distributed throughout the developing and adult CNS (reviewed in (Okaty et al., 2019)), influences a myriad of physiological processes, including mood and anxiety (see reviews by (Berger et al., 2009; Carhart-Harris and Nutt, 2017)). Serotonergic innervation in the brain is derived from cell populations within the raphe nuclei of the brainstem (Muzerelle et al., 2016). 5-HT serves as an integral modulator of processes that form and mature thalamocortical and limbic neurocircuits throughout the developing forebrain (Okaty et al., 2019; Suri et al., 2015). Transgenic (Yadav et al., 2011) or pharmacological (Yu et al., 2014) perturbations of serotonergic signaling in early CNS development thus lead to maladaptive behaviors in adulthood, including altered responses to psychostimulants (*e.g.*, *d*-amphetamine [AMPH]), anxiety-/depressive-like phenotypes, and enhanced sensitivity to environmental stressors (Suri et al., 2015; Daubert and Condron, 2010). For these reasons, serotonergic dysfunction is commonly linked to neuropsychiatric disorders (Nordquist and Oreland, 2010). Consequently, 5-HT-directed drugs (*e.g.*, selective serotonin reuptake inhibitors [SSRIs]) are among the most frequently prescribed psychiatric medications (Pratt et al., 2017). Recreational drugs, such as 3,4-methylenedioxymethamphetamine (MDMA), also target the 5-HT system (Parrott, 2002; Spanos and Yamamoto, 1989). MDMA is most widely recognized as a club drug that gained widespread popularity in the 1990's (Parrott, 2004). Recent revisiting of this drug's utility (Mithoefer et al., 2011; Oehen et al., 2013) suggests that MDMA has significant clinical efficacy as an adjunct to psychotherapy, particularly for post-traumatic stress disorder. Thus, a deeper understanding of the precise mechanisms by which MDMA exerts its complex effects on 5-HT function in the CNS is needed.

The most proximal molecular targets of MDMA are the plasmalemmal monoamine transporters (MATs) (especially the 5-HT transporter (SERT), the dopamine (DA) transporter (DAT), and the norepinephrine transporter). MATs on presynaptic membranes normally mediate neurotransmitter reuptake from the synaptic cleft following neurotransmitter release (Blakely et al., 1994) (for review, see (Uhl and Johnson, 1994; Iversen, 2000)). Although MDMA dose-dependently interacts with each MAT mentioned above, it has highest affinity for SERT (Han and Gu, 2006; Rothman and Baumann, 2003). MDMA is a substrate for SERT and acts as a competitive reuptake inhibitor of endogenous 5-HT – one mechanism by which MDMA elevates extracellular 5-HT (Rudnick and Wall, 1992; Sandtner et al., 2016). Once MDMA is taken up by SERT into presynaptic 5-HT

terminals, the drug facilitates reverse transport by SERT (via multiple complex mechanisms) to ultimately drive 5-HT efflux into the synaptic cleft, thereby further augmenting 5-HT levels (Rudnick and Wall, 1992; Koch and Galloway, 1997; Hilber et al., 2005). The ability of MDMA to markedly increase 5-HT release throughout the brain is required for its unique and diverse effects (Liechti et al., 2000).

RGS proteins principally accelerate the termination of heterotrimeric G protein signaling downstream of GPCR activation (*i.e.*, exerting GTPase-accelerating protein [GAP] activity) via the highly conserved Gα-interacting RGS domain (Soundararajan et al., 2008). RGS12, a member of the Regulator of G protein Signaling (RGS) protein superfamily (Snow et al., 1998; Snow et al., 1997), is abundantly expressed in the embryonic nervous system (Martin-McCaffrey et al., 2005), and it displays appreciable protein expression within some serotonergic projection regions of the adult mouse brain (*e.g.*, cortex, hippocampus, striatum, midbrain) (Gross et al., 2018; Gross et al., 2019). We have previously shown that stimulation of hyperlocomotion by acute administration of DAT-targeting psychostimulants (AMPH, cocaine) is reduced in RGS12-null mice (Gross et al., 2018). Moreover, these mice exhibit brain region-specific alterations in DAT expression and function. Given these previous observations that RGS12 is required for normal responses to DAT-targeting psychostimulants, we sought to determine whether RGS12 also plays a role in MDMA-induced hyperlocomotion, SERT expression/function, and/or serotonergically modulated behaviors.

Methods

Animals

Generation of *Rgs12*$^{\Delta 5-8/\Delta 5-8}$ mice on a C57BL/6J background was previously described (Gross et al., 2018). Male and female mice were generated by heterozygous breedings and housed under standard temperature, humidity, and lighting (12 hours light / 12 hours dark; lights on at 6:00am). All behavioral experiments and tissue procurements were performed during the light cycle using mice between 8–10 weeks of age. All mice were provided food and water *ad libitum*. All experiments were conducted in accordance with approved protocols from the West Virginia University and Duke University Animal Care and Use Committees and followed the National Institute of Health guidelines for use of animals in research. Procedures for the behavioral assays are described below and were conducted according to previously published methods (as cited). Mice were used for only one behavioral assay involving acute drug dosing. More specifically, all drug-based studies were performed with drug-naïve mice. Thus, there was no sequence of multiple, drug-based experimental trials to define for individual mice used in this study.

MDMA-stimulated locomotor activity

Open-field locomotor activity was evaluated at WVU using 16 × 16 photobeam activity system (PAS) chambers from San Diego Instruments, San Diego, CA (enclosure dimensions of 16” (w) × 16” (d) × 15” (h)) under standard environmental conditions and as previously described (Gross et al., 2018). Horizontal locomotor activity was measured as total X and Y coordinate beam-breaks collected in 5-min bins. Acute MDMA-induced locomotor

activity experiments were conducted after two days of acclimation to the open-field chamber. On day 1, RGS12-null mice and wild-type littermate controls were habituated to the locomotor chambers over 150 min to reduce the influence of novelty on subsequent testing. On day 2, all mice were placed into the locomotor chambers for 30 min before a control, intraperitoneal (ip) administration of saline (0.9% NaCl at 10 ml/kg final volume); locomotor activity was measured subsequently over 80 min. On day 3, mice were placed again into the locomotor chambers for 30 min and then injected with MDMA (10 or 30 mg/kg, dissolved in saline at 10 ml/kg final volume, ip; see (Doly et al., 2008)). MDMA-induced hyperlocomotion was then monitored over 80 min. MDMA was obtained from Cayman Chemical Co. (Ann Arbor, MI); all other drugs used in this study were obtained from Sigma-Aldrich (St. Louis, MO) or Tocris (Minneapolis, MN).

High-performance liquid chromatography with electrochemical detection (HPLC-ECD)

Dissected, 5-HT-enriched brain regions (whole cerebral cortex or "cortex," hippocampus, midbrain, ventral striatum, and dorsal striatum) from RGS12-null and wild-type littermate control mice were snap-frozen in a dry-ice/ethanol bath. Subsequent HPLC-ECD measurements of 5-HT and its metabolite 5-HIAA were performed in collaboration with the Vanderbilt VBI Neurochemistry Core using published procedures (Ye et al., 2014; Ye et al., 2015; Oliver et al., 2016; Dohn et al., 2017).

[^{3}H]Citalopram saturation binding to SERT

SERT saturation binding experiments, conducted to determine whether mice exhibited differential SERT protein levels/binding sites, were performed as previously described (Doly et al., 2008) with minor modifications. Briefly, several SERT-expressing brain regions were rapidly dissected from RGS12-null and wild-type littermate control mice and frozen on dry ice. All procedures were carried out at 0 – 4 °C unless otherwise denoted. Brain tissues were separately homogenized with a Polytron homogenizer with 10 volumes of transporter binding buffer (50 mM Tris-HCl pH 7.4, 120 mM NaCl, and 5 mM $MgCl_2$). Homogenates were then centrifuged at 20,800 × *g* for 20 min. The resulting pellet was then resuspended in transporter binding buffer and added to tubes containing [^{3}H]citalopram (Perkin-Elmer, Waltham, MA) (0.63 to 20 nM final concentrations) and incubated for 1 hr at room temperature; nonspecific binding was determined in the presence of 10 μM cold citalopram. Binding reactions were filtered through 0.1% polyethylenimine (PEI)-soaked Whatman GF/B filters using a Brandel harvester. After three rapid washes with ice-cold transporter binding buffer, the resulting filter discs were analyzed by liquid scintillation counting in EcoScint A cocktail. Curves of specific [^{3}H]citalopram binding (*i.e.*, total [^{3}H]citalopram binding - non-specific [^{3}H]citalopram binding) were fit using nonlinear regression (GraphPad Prism 8) to determine maximal binding (B_{max}) and dissociation constant (K_d) values.

[^{3}H]5-HT uptake and MDMA-induced [^{3}H]5-HT efflux in synaptosomes

For [^{3}H]5-HT uptake experiments, synaptosomes were prepared by homogenizing brain-region tissues (pooled from three mice per genotype) in 10 volumes of ice-cold sucrose buffer (10% sucrose, 5 mM HEPES pH 7.4) with a Potter-Elvehjem homogenizer (10 strokes). All procedures were carried out at 0 – 4 °C unless otherwise denoted. Homogenates

were centrifuged at 1,000 × *g* for 10 min, and supernatants containing crude synaptosomes were maintained on ice. Synaptosomes were then added to tubes containing Krebs-Ringer uptake buffer (120 mM NaCl, 20 mM Tris-HCl pH 7.4, 5 mM KCl, 1.2 mM $MgSO_4$, 2.5 mM $CaCl_2$, 10 mM glucose, 1 mM ascorbic acid, and 0.1 mM pargyline [an MAO inhibitor]) plus [^{3}H]5-HT (14.2 μM, Perkin-Elmer) and incubated for 10 min at room temperature. Non-specific [^{3}H]5-HT uptake was determined in the presence of 10 μM cold citalopram and subtracted from total uptake. Uptake reactions were filtered through 0.1% PEI-soaked Whatman GF/B filters using a Brandel harvester. After washing the filters three times with ice-cold Krebs-Ringer buffer, synaptosomal [^{3}H]5-HT content was measured by liquid scintillation counting in EcoScint A cocktail. Specific [^{3}H]5-HT uptake curves were fit using nonlinear regression (Prism 8) to determine the maximum rate (V_{max}) and Michaelis-Menten constant (K_m) values.

MDMA-induced [^{3}H]5-HT efflux assays were performed as previously described (Rothman et al., 2001). Briefly, synaptosomes were prepared as described above but with ice-cold sucrose buffer supplemented with 1 μM reserpine (VMAT2 inhibitor), 100 nM GBR12935 (DAT-specific inhibitor), and 100 nM nomifensine (DAT/NET inhibitor). GBR12935 and nomifensine were added to the buffer in order to prevent non-specific uptake of [^{3}H]5-HT through DAT and NET, respectively (Rothman et al., 2001). Synaptosomes were then preloaded by incubating them for 60 min with 5 nM [^{3}H]5-HT in uptake buffer (0.5 mM Na_2SO_4, 0.5 mM KH_2PO_4, 126 mM NaCl, 2.4 mM KCl, 0.83 mM $CaCl_2$, 0.8 mM $MgCl_2$, 11.1 mM glucose, 50 μM pargyline, 1 mg/mL ascorbic acid, pH 7.4) supplemented with 1 μM reserpine, 100 nM GBR12935, and 100 nM nomifensine. Following preloading, 450 μl of preloaded synaptosomes were added to tubes containing MDMA (0.1 μM to 10 μM) in Krebs-Ringer buffer. The release reactions proceeded for 5 min and were terminated by addition of 3 ml of ice-cold wash buffer (10 mM Tris-HCl pH 7.4, 0.9% NaCl), followed by rapid filtration through 0.1% PEI-soaked Whatman GF/B filters using a Brandel harvester. Filters were rapidly washed three times with ice-cold wash buffer, and synaptosomal [^{3}H]5-HT content was measured via liquid scintillation counting in EcoScint A cocktail. [^{3}H]5-HT release data were fit using nonlinear regression (Prism 8) to determine maximal efficacy (E_{max}) and half-maximal effective concentration (EC_{50}) values.

Quantitative reverse transcription-polymerase chain reaction (qRT-PCR) analysis of Slc6a4, Tph2, and Fev steady-state mRNA levels

To obtain raphe-containing brain tissue, four cuts per brain were made, as shown in Supplemental Fig. S1. Total RNA was extracted from dissected tissues using an RNeasy Protect Kit (Qiagen) following the manufacturer's protocol. First-strand cDNA was prepared from RNA using a QuantiTect Reverse Transcription Kit (Qiagen) according to the manufacturer's instructions. qPCR reactions were prepared and run on a Rotor Gene Q (Qiagen) using a QuantiTect SYBR Green PCR Kit (Qiagen) as instructed by the manufacturer. To assess steady-state levels of *Slc6a4*, *Tph2*, *Fev*, *Rn18s*, and *Tubb2* mRNA, QuantiTect Primer Assays (Qiagen) were used (catalog numbers QT00163345, QT00125265, QT00265167, QT02448075, and QT01060283, respectively). The $2^{-\Delta\Delta Ct}$ method (Livak and Schmittgen, 2001) was applied to the qPCR data to calculate fold change in steady-state *Slc6a4*, *Tph2*, and *Fev* mRNA levels as a function of genotype using

steady-state levels of *Rn18s* mRNA as a comparator. Similar results were obtained using steady-state levels of *Tubb2* mRNA as a comparator.

8-OH-DPAT-induced hypothermia

The procedure described by Diaz and colleagues (Diaz et al., 2012) was followed, with minor modifications. Rectal temperatures, before and after ip administration of 8-OH-DPAT, were measured using a J/K/T thermocouple and a lubricated RET-3 probe (Kent Scientific). Mice were acclimated to the testing room for one hour prior to assay. To establish a steady baseline, four measurements per mouse were taken at ten-minute intervals. Afterwards, 8-OH-DPAT (0.5 mg/kg; dissolved in sterile saline solution) was injected ip, and four measurements per mouse were taken at ten-minute intervals.

Behavioral analyses

Open-field locomotion ––—Novelty-induced open-field locomotor activity was assessed at WVU by placing naive RGS12-null and wild-type littermate control mice into PAS chambers (described above) under standard environmental conditions. Horizontal locomotion was monitored for 110 min and quantified as the sum of the total X and Y coordinate beam-breaks collected in 5-min bins. Each PAS apparatus was cleaned between subjects using a water-moistened cloth.

Home-cage locomotion ––—Spontaneous home-cage locomotor activity (*i.e.*, activity in a non-stressful environment) was assessed at WVU using singly housed mice. Mice were acclimated to the testing room for one hour. Then, home-cage locomotor activity was video recorded and tracked for distance traversed over 20 min using ANY-maze software (Stoelting).

Forced swim test (FST) ––—The procedure described by Can and colleagues (Can et al., 2012) was conducted at WVU. RGS12-null and wild-type littermate control mice were acclimated to the testing room for 1 hour. A cylindrical tank (30 cm high × 20 cm diameter) was filled with a volume of water at room temperature sufficient to achieve a depth of 15 cm; a water-resistant infrared thermometer was used to verify the temperature. A video camera was placed to the side of the apparatus and was used to record the behavior of the animal in the tank. Mice were separately held by the tail and slowly placed into the water. Once each mouse was in the water, it was slowly released and monitored (by video camera and by an observer) for 6 min, with only the last 4 min analyzed for the total amount of time the mouse was inactive.

Tail-suspension test (TST) ––—Tail suspension tests (Steru et al., 1985) were conducted at WVU following a previously established procedure (Braida et al., 2009; Kinsey et al., 2007). Briefly, RGS12-null and wild-type littermate control mice were acclimated to the test room for 1 hr. Individual mice were suspended from a flat, horizontal bar 40 cm above the table with adhesive tape placed 1 cm from the tip of the tail. Mice were each suspended for 6 min; the total time each mouse struggled was hand-scored by a blinded observer using video and ANY-maze tracking software (Stoetling Co., Wood Dale, IL). Although tail climbing

has been previously reported in C57BL/6 mice using a round bar (Mayorga and Lucki, 2001), no tail climbing was observed in the present study.

Elevated plus maze (EPM) ––—The protocol described by Walf and Frye (Walf and Frye, 2007) was followed at WVU. Briefly, RGS12-null and wild-type littermate control mice were acclimated to a dimly lit room (50–60 lux) housing the black plastic apparatus, consisting of four arms (two open arms and two arms enclosed by 15.25 cm-high walls) 30 cm long and 5 cm wide, mounted 40 cm off the worktable. Mice were initially placed in the center of the maze facing an open arm and allowed to ambulate over 5 min. Video tracking (ANY-maze; Stoelting) was used to automatically collect arm time data from a digital camera mounted overhead.

Elevated zero maze (EZM) ––—We also performed EZM tests at Duke University, given that some have argued that the elevated zero maze may be superior to the EPM in modeling the anti-anxiety activity of established anxiolytics (Kulkarni et al., 2007; Shepherd et al., 1994). EZM tests were performed as previously described (Fukui et al., 2007). Briefly, an annular maze containing two closed and two open quadrants was surrounded by black curtains and illuminated by 50–60 lux. RGS12-null or wild-type littermate control mice were placed into a closed quadrant and allowed to freely explore the apparatus for 5 min. Responses were recorded by a video camera suspended above the apparatus and analyzed by EthoVision XT software version 9 (Noldus Information Technology, Leesburg, VA). Percent open arm time was computed for each genotype.

Social interaction test ––—Sociability was evaluated at Duke University using methods previously described (Bey et al., 2018). First, an RGS12-null or wild-type littermate control mouse was placed into the center of a test chamber containing two identical, non-social stimuli (“non-social stimulus 1” [NS1] and “non-social stimulus 2” [NS2]) enclosed within wire-mesh containers located on opposite sides of the apparatus. After 10 min, the test mouse was removed from the chamber and one non-social stimulus (NS) was replaced with an adult female C3H/HeJ mouse (Stock No. 000659; Jackson Lab, Bar Harbor, ME) that was confirmed to not be in estrous. The test mouse was then returned to the apparatus and was given free access to the remaining NS and the novel social stimulus (S1) for 10 min. All behaviors were filmed, transferred to Media Player (Noldus Information Technology, Leesburg, VA), and scored using Ethovision software with center and nose-point tracking (Noldus). To calculate a social preference score, the time spent with one stimulus (NS1 or S1) was subtracted from the time spent with the other stimulus (NS2 or NS, respectively) and divided by the total time spent with both stimuli. Positive scores indicated that mice display a preference for S1 relative to NS, whereas negative scores signified a preference for NS. A score of “0” indicated no preference. Data were normalized for each mouse by subtracting the baseline preference score (NS1-NS2) from the novel social stimulus preference score (NS-S1).

Statistics

All data are presented as the mean ± SEM. Statistical significance was set at $p < 0.05$ for all experiments, and data were analyzed by Student’s *t*-test or two-way ANOVA followed

by Sidak's *post hoc* test where appropriate. Shapiro-Wilk tests were performed to evaluate normality ($p > 0.05$) for each behavioral experiment, and Mann-Whitney U tests were used to determine significance for non-parametric data. [^{3}H]5-HT efflux, [^{3}H]5-HT uptake, and [^{3}H]citalopram binding data points for samples from each genotype were fit to the appropriate mathematical model, and nonlinear regression analysis was performed using Prism 8; for each pair of curves, best-fit values were tested for statistically significant difference using F-tests.

Results

RGS12 loss affects MDMA-induced hyperlocomotion after open-field acclimation

Given prior observations that RGS12-null mice exhibit attenuated hyperlocomotion to amphetamine or cocaine (Gross et al., 2018), we first investigated whether RGS12-null mice displayed a similar decreased response to the serotonergic psychostimulant MDMA. After a first-day's exposure to an open-field locomotion chamber to acclimate each individual mouse to this novel environment, mice of both genotypes (RGS12-null and wild-type littermate controls) exhibited equivalent locomotion, both before and after a control, saline injection (Fig. 1a; two-way ANOVA effects of genotype not significant: $F_{1,44} = 0.025$, $p = 0.876$ over first 30 min, and $F_{1,44} = 0.47$, $p = 0.497$ over subsequent 60 min). Mice of both genotypes also exhibited equivalent locomotion over the first thirty minutes of exposure to the same open-field locomotion chamber on the third day (Fig. 1b,c; two-way ANOVA effects of genotype not significant: $F_{1,43} = 1.4$, $p = 0.244$ over first 30 min prior to 10 mg/kg MDMA, and $F_{1,43} = 0.05$, $p = 0.831$ over first 30 min prior to 30 mg/kg MDMA). However, on the third day, following acute administration of 10 mg/kg MDMA, RGS12-null mice exhibited markedly reduced locomotion over 60 min relative to wild-type littermate controls (Shapiro-Wilk $W = 0.933$, $p = 0.012$; Mann-Whitney $U = 63.50$, $p < 0.0001$; Fig. 1b *inset*). Repeated-measures two-way ANOVA of locomotor activity over these 60 min revealed an effect of genotype ($F_{1,43} = 23.9$, $p < 0.0001$), time ($F_{11,473} = 7.8$, $p < 0.0001$), and a genotype × time interaction ($F_{11,473} = 5.1$, $p < 0.0001$). In contrast, RGS12-null mice exhibited similar locomotor activity over 60 min following a higher dose (30 mg/kg) of MDMA relative to wild-type littermate controls ($t_{43} = 1.5$, $p = 0.148$; Fig. 1c *inset*). Repeated-measures two-way ANOVA of locomotor activity following acute administration of 30 mg/kg MDMA (Fig. 1c) revealed no effect of genotype ($F_{1,43} = 1.8$, $p = 0.191$), but effects of time ($F_{17,731} = 104.7$, $p < 0.0001$) and a genotype × time interaction ($F_{17,731} = 3.0$, $p < 0.0001$) were significant. To control for any inherent changes to spontaneous locomotor activity that may arise upon RGS12 loss, singly housed mice of both genotypes were observed in a non-stressed, home-cage environment. No significant difference in locomotor behavior was found between the genotypes (Kolmogorov-Smirnov nonparametric, unpaired t-test: $p = 0.60$; Fig. 1d).

Investigations of 5-HT, 5-HIAA, and SERT levels in the brains of RGS12-null mice

Steady-state levels of 5-HT, 5-HIAA, and 5-HT turnover—To determine if homeostatic levels of 5-HT or its major metabolite 5-hydroxyindoleacetic acid (5-HIAA) were altered in the absence of RGS12 expression, we performed HPLC-ECD analysis on several 5-HT-rich brain regions (cortex, hippocampus, midbrain, ventral striatum, and dorsal

striatum) from RGS12-null and wild-type mice. These analyses revealed that RGS12-null mice contain increased levels of 5-HT in the cortex (Fig. 2a(i); $t_9 = 2.6$, p = 0.027) and hippocampus (Fig. 2b(i); $t_{10} = 2.2$, p = 0.044), but not in the midbrain, ventral striatum, or dorsal striatum (Fig. 2c–e(i); p > 0.05). Levels of the 5-HT metabolite 5-HIAA did not differ between genotypes in any brain regions tested (Fig. 2a–e(ii); p > 0.05). Calculation of the 5-HIAA to 5-HT ratio as an index of metabolic activity (Rothman et al., 2001) suggested that RGS12 loss does not significantly affect 5-HT metabolism in any brain regions assayed (Fig. 2a–e(iii)). However, a notable trend for increased 5-HT turnover was observed in the midbrain (Fig. 2c(iii); $t_{10} = 2.0$, p = 0.068).

Steady-state levels of SERT binding sites—Mice lacking SERT expression exhibit locomotor insensitivity to MDMA (Bengel et al., 1998), supporting the idea that changes in SERT expression and/or function might underlie the altered MDMA-induced hyperlocomotion we observed in RGS12-null mice. To ascertain whether RGS12 loss results in any alteration of steady-state SERT protein levels, we performed [^{3}H]citalopram saturation binding assays (Fig. 3) using membrane preparations from the cortex, hippocampus, midbrain, ventral striatum, and dorsal striatum of RGS12-null mice and wild-type littermate controls. RGS12-null mice exhibited an increased number of SERT binding sites (B_{max}) in the cortex (Fig. 3a; $F_{1,44} = 29.9$, p < 0.0001) and midbrain (Fig. 3c; $F_{1,67} = 20.3$, p < 0.0001) – namely, the two regions with the highest SERT expression among the subset of brain regions surveyed. RGS12-null mice were also found to have a slight decrease in SERT B_{max} in the hippocampus compared to wild-type controls (Fig. 3b; $F_{1,44} = 10.5$, p = 0.002). By comparison, B_{max} measurements were similar for the ventral striatum (Fig. 3d; $F_{1,68} = 1.9$, p = 0.165) and dorsal striatum (Fig. 3e; $F_{1,44} = 3.4$, p = 0.070) of RGS12-null mice compared with wild-type controls. The affinity of [^{3}H]citalopram for SERT (K_d) in the hippocampus was significantly different between genotypes ($F_{1,44} = 7.4$, p = 0.009); however, the K_d values did not differ between genotypes in any of the other brain regions tested. The B_{max} and K_d values for all brain regions tested are summarized in Table 1.

SERT function is altered in brain regions of RGS12-null mice

SERT-specific [^{3}H]5-HT uptake—To determine whether RGS12-null mice exhibit alterations in SERT function, we performed [^{3}H]5-HT uptake analyses using brain region-derived synaptosomal preparations pharmacologically treated to isolate SERT function (Fig. 4i), as previously described (Doly et al., 2008). Synaptosomes from the cortex (Fig. 4a(i); $F_{1,103} = 13.5$, p = 0.0004) and the midbrain (Fig. 4c(i); $F_{1,92} = 14.4$, p = 0.0003) of RGS12-null mice exhibited increased, SERT-specific, [^{3}H]5-HT uptake (V_{max}), consistent with the observations of increased SERT B_{max} in these regions (Fig. 3a,c). In addition, elevated SERT V_{max} was observed in synaptosomes from the ventral striatum of RGS12-null mice (Fig. 4d(i); $F_{1,66} = 14.6$, p = 0.0003), despite no observed difference in SERT B_{max} in this region between the two genotypes (Fig. 3d). By contrast, [^{3}H]5-HT uptake was similar in synaptosomes from the hippocampus (Fig. 4b(i); $F_{1,56} = 0.004$, p = 0.944) and dorsal striatum (Fig. 4e(i); $F_{1,48} = 0.003$, p = 0.955) of RGS12-null and wild-type mice. The affinities of [^{3}H]5-HT for SERT (K_m values) did not differ between genotypes across all

five brain regions tested ($p > 0.05$). The V_{max} and K_m values for all brain regions tested are summarized in Table 1.

MDMA-induced [^{3}H]5-HT efflux—MDMA elevates extracellular 5-HT levels primarily by stimulating SERT-mediated 5-HT efflux (*i.e.*, creating conditions for SERT reverse transport) (Rudnick and Wall, 1992; Crespi et al., 1997). Given that mice lacking SERT do not display hyperlocomotion in response to MDMA administration (Bengel et al., 1998), locomotor responses to MDMA are likely dependent, at least in part, on MDMA-induced 5-HT efflux through SERT. To evaluate whether the alterations to MDMA-induced hyperlocomotion in RGS12-null mice (Fig. 1) are associated with differences in MDMA-induced 5-HT efflux, we performed MDMA-stimulated [^{3}H]5-HT efflux assays with preloaded, brain-region synaptosomes from RGS12-null and wild-type mice, as previously described (Rothman et al., 2001). DAT and NET inhibitors (*i.e.*, GBR12935 and nomifensine) were co-incubated with [^{3}H]5-HT during synaptosome preloading to prevent [^{3}H]5-HT uptake through DAT and NET, respectively (Rothman et al., 2001). Slight decreases in the maximal efficacy (E_{max}) of MDMA in stimulating [^{3}H]5-HT efflux were observed in cortical (Fig. 4a(ii); $F_{1,178} = 6.8$, $p = 0.009$) and midbrain (Fig. 4c(ii); $F_{1,159} = 12.6$, $p = 0.0005$) synaptosomes of RGS12-null mice as compared with those of their wild-type littermates. By comparison, no genotype differences were discerned in synaptosomes from the hippocampus (Fig. 4b(ii); $F_{1,76} = 0.1$, $p = 0.743$), ventral striatum (Fig. 4d(ii); $F_{1,132} = 2.5$, $p = 0.114$), or dorsal striatum (Fig. 4e(ii); $F_{1,77} = 0.5$, $p = 0.476$). The potency (EC_{50}) by which MDMA elicited [^{3}H]5-HT efflux from preloaded synaptosomes did not differ between genotypes in any of the five brain regions tested. The E_{max} and pEC_{50} values for all brain regions tested are summarized in Table 1.

RGS12 loss does not affect midbrain *Slc6a4, Tph2* or *Fev* mRNA levels, or 5-HT$_{1A}$ receptor signaling

Given the brain-region-specific effect of RGS12 loss on [^{3}H]citalopram binding sites and [^{3}H]5-HT uptake activity, we measured the steady-state levels of SERT-encoding mRNA (*Slc6a4*). In the adult brain, *Slc6a4* mRNA is expressed predominantly in the raphe. As such, we dissected raphe-containing tissue from the brains of RGS12-null and wild-type littermates and extracted RNA for subsequent qRT-PCR analysis. As shown in Fig. 5a, steady-state levels of *Slc6a4* mRNA did not differ significantly between tissue from *Rgs12* knockout and wild-type mice. Contemporaneously, we measured steady-state levels of *Tph2* (the gene encoding brain-specific tryptophan hydroxylase) and *Fev* (the gene encoding the Pet-1 transcription factor) mRNAs – commonly assessed markers of serotonergic neurons. As shown in Fig. 5a, steady-state levels of *Tph2* and *Fev* did not differ significantly between tissue from *Rgs12* knockout and wild-type mice.

As the GAP activity of RGS12 is known to oppose signaling from activated GPCRs coupled to heterotrimeric Gi/o proteins (*e.g.*, (Snow et al., 1998; Soundararajan et al., 2008; Gross et al., 2019)), a simple explanation for the observed behavioral and biochemical phenotypes of *Rgs12* knockout mice could be a resultant sensitization of Gi/o-coupled GPCRs to agonist stimulation. To test this possibility for the serotonin 5-HT$_{1A}$ receptor, we treated RGS12-null mice and wildtype littermate controls with 8-hydroxy-2-(di-*n*-propylamino)tetralin

(8-OH-DPAT) and measured their rectal temperatures in 10-minute intervals. No genotype-associated difference in 8-OH-DPAT-induced hypothermia was observed (Fig. 5b).

RGS12 loss disrupts serotonergically modulated behaviors

Observations of altered SERT expression (Fig. 3) and 5-HT uptake (Fig. 4) in RGS12-null mice suggest that the loss of RGS12 expression leads to basal disruptions to serotonergic neurotransmission in adult mice (*i.e.*, even under drug-independent conditions). 5-HT is recognized as an integral modulator of many clinically relevant behavioral responses, including stress-coping/depression-like behavior (for review, see (Meltzer, 1990; Owens and Nemeroff, 1994; Nutt, 2002)) and anxiety-like behavior (Holmes et al., 2003b; Kalueff et al., 2007; Mosienko et al., 2012). To evaluate whether RGS12 loss is sufficient to disrupt any of these processes, we conducted a battery of behavioral assays related to each of these serotonergically modulated behavioral outcomes (Fig. 6). We first evaluated open-field locomotor activity in RGS12-null and wild-type littermate control mice. We found that RGS12-null mice had reduced locomotion in a novel environment relative to wild-type controls (Fig. 6a). To assess stress-coping/depression-like behavior, we used the forced swim test (FST) and the tail suspension test (TST) (Castagne et al., 2011). In both assays, RGS12-null mice exhibited reduced immobility relative to wild-type controls (FST: Fig. 6b; $t_{39} = 3.7$, p = 0.0005) (TST: Fig. 6c; $t_{13} = 2.1$, p = 0.049). These findings suggest that RGS12-null mice exert an active stress-coping strategy and display an anti-depressive-like phenotype in these assays, consistent with responses produced by acute administration of an SSRI anti-depressant to elevate serotonin levels (Holmes et al., 2002).

To evaluate anxiety-like behavior, we tested RGS12-null mice in the elevated plus maze (EPM) and elevated zero maze (EZM) (Shepherd et al., 1994; Walf and Frye, 2007). RGS12-null mice showed decreased open arm time in both assays (EPM: Fig. 6d; $t_{22} = 3.3$, p = 0.002) (EZM: Fig. 6e; $t_{34} = 2.2$, p = 0.029), suggesting that these mice exhibit an anxiety-like phenotype. An examination of sociability/social interaction revealed that the RGS12-null mice spent reduced time with a novel social stimulus *versus* a non-social stimulus relative to wild-type mice (Fig. 6f; $t_{39} = 2.4$, p = 0.020). RGS12-null mice and their wild-type littermates did not differ in their baseline preference for non-social stimuli ($t_{39} = 1.1$, p = 0.226; RGS12-null = −0.058 ± 0.047, wild-type = 0.038 ± 0.063). Taken together, these behavioral data suggest that constitutive loss of RGS12 alters serotonergic function sufficiently to manifest disruptions in several serotonergically modulated behaviors in adult mutant mice.

Discussion

The key findings from this study are that RGS12 loss leads to (i) reduced hyperlocomotion when administered a low dose of MDMA, (ii) increased, brain region-specific, SERT expression and 5-HT uptake, and (iii) increased anxiety-like and anti-depressive-like behaviors. These findings suggest that RGS12 expression is required to establish and/or maintain the proper function of specific serotonergic regions/circuits in adult mice. SERT knockout mice exhibit neither hyperlocomotion (Bengel et al., 1998) nor augmented extracellular 5-HT levels (Hagino et al., 2011) following administration of low-to-moderate

doses of MDMA. Additionally, mice constitutively lacking the transcription factor Pet-1 – encoded by *Fev* and required for proper development of CNS serotonergic circuitry (Hendricks et al., 1999) -- fail to display hyperlocomotion upon administration of 5 or 10 mg/kg MDMA (Yadav et al., 2011; Kiyasova et al., 2011). Notably, synaptosomes from these Pet-1-null knockout mice exhibit comparable MDMA-induced [^{3}H]5-HT efflux to synaptosomes from control mice when normalized for their deficient [^{3}H]5-HT preloading capacity (Kiyasova et al., 2011). Taken together, these prior reports indicate that a loss of MDMA-induced hyperlocomotion can occur (1) independent of concomitant disruptions in MDMA-evoked 5-HT efflux and (2) following neurodevelopmental perturbation of 5-HT signaling/circuitry. In light of these previous findings, we suspect that the lack of hyperlocomotion to a low dose of MDMA in RGS12-null mice could be related to altered connectivity of serotonergic neurons with some or all of their targets, changes in the morphology of serotonergic neurons (*e.g.*, axon branch development; (Deneris and Gaspar, 2018), and/or differential biochemistry (*e.g.*, increased SERT expression and 5-HT uptake). The lack of hyperlocomotion in response to MDMA in RGS12-null mice does not seem to be dependent upon changes in MDMA-induced 5-HT efflux, as synaptosomes from RGS12-null mice fail to exhibit appreciable alterations in MDMA-induced [^{3}H]5-HT efflux. Notably, the observed increase in SERT expression does not correspond with alteration in *Slc6a4* mRNA levels, suggesting a post-translational mechanism.

Enhanced SERT expression and SERT-mediated 5-HT uptake capacities in the cortex, midbrain, and ventral striatum of RGS12-null mice may enable more efficient clearance of extracellular 5-HT *in vivo*. This circumstance would lead to reduced hyperlocomotion following administration of 10 mg/kg MDMA -- especially if this dose of MDMA does not saturate SERT in these mice. By comparison, higher doses of MDMA likely saturate all, or nearly all of, SERT in RGS12-null mice, thereby precluding their increased reuptake capacity and thus normalizing hyperlocomotor responses to those of wild-type controls. This hypothesis is consistent with our prior observations that RGS12-null mice show reduced hyperlocomotion to low-to-moderate doses of the DAT-targeting psychostimulant AMPH, display enhanced DAT expression and [^{3}H]DA uptake (in ventral, but not dorsal, striatum), and exhibit only a mild attenuation of AMPH-induced [^{3}H]DA efflux potency in ventral striatal synaptosomes (Gross et al., 2018). Together, these prior and current findings provide support for the idea that RGS12 loss reduces hyperlocomotion to low-to-moderate doses of psychostimulants (*e.g.*, AMPH, cocaine, MDMA), at least in part, through enhanced transporter (*i.e.*, DAT, SERT) expression and/or transporter-mediated monoamine neurotransmitter clearance in combination with mildly dysfunctional transporter-mediated DA/5-HT efflux (Gross et al., 2018). Evidence that 8-OH-DPAT-induced hypothermia is unchanged in RGS12-null mice (Fig. 2) does suggest that no alteration has occurred in the function of raphe somatodendritic 5-HT$_{1A}$ autoreceptors (Higgins et al., 1988).

Our study has also revealed that RGS12-null mice display several aberrant, serotonergically modulated behavioral phenotypes under drug-naïve conditions. Acute administration of SSRIs or chemogenetic activation of serotonergic raphe neurons each recapitulates the behavioral phenotypes that we observed in RGS12-null mice -- namely, reduced open-field exploration and increased anti-depressive- and anxiety-like behaviors (Teissier et al., 2015). Thus, it is possible that RGS12-null mice tonically and/or phasically (*e.g.*, under conditions

of environmental stress) exhibit elevated serotonergic neurotransmission, thereby resulting in attenuated responses to novelty (*e.g.*, to an open field, to novel social stimuli), in anxiety-like behaviors, and in anti-depressive-like behaviors. Early developmental periods are particularly sensitive to perturbations in serotonergic homeostasis. For example, transgenic over-expression of SERT in mice engenders anti-anxiety-like/depressive-like phenotypes in adulthood (Jennings et al., 2006; Line et al., 2011). Conversely, SSRI exposure during early postnatal development (Ansorge et al., 2004; Ansorge et al., 2008) or constitutive SERT deletion (Kalueff et al., 2007; Holmes et al., 2003a; Lira et al., 2003) (both of which augment serotonergic tone) each leads to "paradoxical" anxiety-like and depressive-like behavioral phenotypes in adult mice (reviewed in (Suri et al., 2015)). Based on the four lines of evidence enumerated below, we suspect that RGS12 plays a key role in serotonergic signaling during early, sensitive periods of CNS development, particularly in processes and within CNS regions integral for determining the sensitivity and/or maturation of cortical and limbic circuits that underlie behaviors during adulthood: (1) RGS12 is highly expressed during neurodevelopment (Martin-McCaffrey et al., 2005); (2) *Rgs12* mRNA is abundant in E12.5 serotonergic neurons of rostral and caudal neural tube regions (Supplemental Fig. S2), yet this same level of abundance is not evident in adult dorsal raphe or median raphe neurons (Supplemental Fig. S3); (3) appropriate levels of RGS12 expression are required for proper axonogenesis in primary neurons (*e.g.*, dorsal root ganglia) (Willard et al., 2007); and (4) RGS12 expression is altered following neurodevelopmental perturbations (*e.g.*, whisker-trimming (Butko et al., 2013) or DISC1 overexpression (Sialana et al., 2018)).

Initial studies of *Slc6a4* knockout mice were conducted in CD-1 mice (Bengel et al., 1998). Similar to our finding with RGS12-null mice in the C57BL/6J background, Bengel and colleagues reported that CD-1 mice lacking SERT expression exhibit no locomotor stimulation upon treatment with low-dose MDMA (5 mg/kg – a dose that elicited robust hyperlocomotion in wild-type CD-1 mice). In contrast, *Slc6a4* knockout CD-1, like wild-type control CD-1 mice, exhibit robust hyperlocomotion in response to amphetamine (5 mg/kg) (Bengel et al., 1998). More recently, *Slc6a4* knockout mice on the C57BL/6J background have been described (Kalueff et al., 2007). Kalueff and colleagues found that SERT loss led to "striking reductions in exploration and activity in novelty based tests" (including open-field and novel-object-recognition tests). Further, Kalueff *et al.* observed that C57BL/6J mice lacking SERT exhibited "markedly reduced" sociability compared with wild-type C57BL/6J mice, similar to our findings with RGS12 loss.

In summary, constitutive loss of RGS12 in mice disrupts both basal and pharmacologically evoked serotonergic signaling and serotonergically modulated behavior. We recently identified the mechanism by which RGS12 modulates DAT expression/function: *i.e.*, differential effects on the heterotrimeric G protein and β-arrestin signaling pathways originating from kappa opioid receptor (KOR) activation (Gross et al., 2019). As dynorphin in the ventral striatum can elicit local stimulation of serotonin reuptake (Schindler et al., 2012), and KOR ligands can also modulate SERT function (Sundaramurthy et al., 2017), it is possible that the effects of RGS12 on SERT expression/function are similarly mediated by KOR or another GPCR.

Supplementary Material

Refer to Web version on PubMed Central for supplementary material.

Acknowledgments

Funding for these studies was supported in part by R01 DA048153 (to DPS) and R03 DA039335 (to SGK). ANW had predoctoral support from the WVU Behavioral & Biomedical Sciences T32 training grant (NIH T32 GM132494). JDG and SWK each had early predoctoral support from NIH T32 GM081741 and subsequent independent support from a NIDA predoctoral fellowship (NIH F31 DA043331) and a NIDA MD/PhD combined degree fellowship (NIH F30 DA044711), respectively. Some of the behavioral equipment and software at the Duke University Mouse Behavioral and Neuroendocrine Analysis Core Facility was purchased by a grant from the North Carolina Biotechnology Center. We thank Dr. Ramona Rodriguiz (Assistant Director, Duke University Mouse Behavioral and Neuroendocrine Analysis Core Facility) for providing training and advice on EZM and sociability tests.

References

Ansorge MS, Morelli E and Gingrich JA (2008) Inhibition of serotonin but not norepinephrine transport during development produces delayed, persistent perturbations of emotional behaviors in mice. J Neurosci 28(1): 199–207. [PubMed: 18171937]

Ansorge MS, Zhou M, Lira A, et al. (2004) Early-life blockade of the 5-HT transporter alters emotional behavior in adult mice. Science 306(5697): 879–881. [PubMed: 15514160]

Bengel D, Murphy DL, Andrews AM, et al. (1998) Altered brain serotonin homeostasis and locomotor insensitivity to 3, 4-methylenedioxymethamphetamine (“Ecstasy”) in serotonin transporter-deficient mice. Mol Pharmacol 53(4): 649–655. [PubMed: 9547354]

Berger M, Gray JA and Roth BL (2009) The expanded biology of serotonin. Annu Rev Med 60: 355–366. [PubMed: 19630576]

Bey AL, Wang X, Yan H, et al. (2018) Brain region-specific disruption of Shank3 in mice reveals a dissociation for cortical and striatal circuits in autism-related behaviors. Transl Psychiatry 8(1): 94. [PubMed: 29700290]

Blakely RD, De Felice LJ and Hartzell HC (1994) Molecular physiology of norepinephrine and serotonin transporters. J Exp Biol 196: 263–281. [PubMed: 7823027]

Braida D, Capurro V, Zani A, et al. (2009) Potential anxiolytic- and antidepressant-like effects of salvinorin A, the main active ingredient of Salvia divinorum, in rodents. Br J Pharmacol 157(5): 844–853. [PubMed: 19422370]

Butko MT, Savas JN, Friedman B, et al. (2013) In vivo quantitative proteomics of somatosensory cortical synapses shows which protein levels are modulated by sensory deprivation. Proc Natl Acad Sci U S A 110(8): E726–735. [PubMed: 23382246]

Can A, Dao DT, Arad M, et al. (2012) The mouse forced swim test. J Vis Exp. DOI: 10.3791/3638. (59): e3638. [PubMed: 22314943]

Carhart-Harris RL and Nutt DJ (2017) Serotonin and brain function: a tale of two receptors. J Psychopharmacol 31(9): 1091–1120. [PubMed: 28858536]

Castagne V, Moser P, Roux S, et al. (2011) Rodent models of depression: forced swim and tail suspension behavioral despair tests in rats and mice. Curr Protoc Neurosci Chapter 8: Unit 8 10A.

Crespi D, Mennini T and Gobbi M (1997) Carrier-dependent and Ca(2+)-dependent 5-HT and dopamine release induced by (+)-amphetamine, 3,4-methylendioxymethamphetamine, p-chloroamphetamine and (+)-fenfluramine. Br J Pharmacol 121(8): 1735–1743. [PubMed: 9283711]

Daubert EA and Condron BG (2010) Serotonin: a regulator of neuronal morphology and circuitry. Trends Neurosci 33(9): 424–434. [PubMed: 20561690]

Deneris E and Gaspar P (2018) Serotonin neuron development: shaping molecular and structural identities. Wiley Interdiscip Rev Dev Biol 7(1).

Diaz SL, Doly S, Narboux-Neme N, et al. (2012) 5-HT(2B) receptors are required for serotonin-selective antidepressant actions. Mol Psychiatry 17(2): 154–163. [PubMed: 22158014]

Dohn MR, Kooker CG, Bastarache L, et al. (2017) The Gain-of-Function Integrin beta3 Pro33 Variant Alters the Serotonin System in the Mouse Brain. J Neurosci 37(46): 11271–11284. [PubMed: 29038237]

Doly S, Valjent E, Setola V, et al. (2008) Serotonin 5-HT2B receptors are required for 3,4-methylenedioxymethamphetamine-induced hyperlocomotion and 5-HT release in vivo and in vitro. J Neurosci 28(11): 2933–2940. [PubMed: 18337424]

Fukui M, Rodriguiz RM, Zhou J, et al. (2007) Vmat2 heterozygous mutant mice display a depressive-like phenotype. J Neurosci 27(39): 10520–10529. [PubMed: 17898223]

Gross JD, Kaski SW, Schmidt KT, et al. (2019) Role of RGS12 in the differential regulation of kappa opioid receptor-dependent signaling and behavior. Neuropsychopharmacology Epub ahead of print 2019/05/30. DOI: 10.1038/s41386-019-0423-7.

Gross JD, Kaski SW, Schroer AB, et al. (2018) Regulator of G protein signaling-12 modulates the dopamine transporter in ventral striatum and locomotor responses to psychostimulants. J Psychopharmacol 32(2): 191–203. [PubMed: 29364035]

Hagino Y, Takamatsu Y, Yamamoto H, et al. (2011) Effects of MDMA on Extracellular Dopamine and Serotonin Levels in Mice Lacking Dopamine and/or Serotonin Transporters. Curr Neuropharmacol 9(1): 91–95. [PubMed: 21886569]

Han DD and Gu HH (2006) Comparison of the monoamine transporters from human and mouse in their sensitivities to psychostimulant drugs. BMC Pharmacol 6: 6. [PubMed: 16515684]

Hendricks T, Francis N, Fyodorov D, et al. (1999) The ETS domain factor Pet-1 is an early and precise marker of central serotonin neurons and interacts with a conserved element in serotonergic genes. J Neurosci 19(23): 10348–10356. [PubMed: 10575032]

Higgins GA, Bradbury AJ, Jones BJ, et al. (1988) Behavioural and biochemical consequences following activation of 5HT1-like and GABA receptors in the dorsal raphe nucleus of the rat. Neuropharmacology 27(10): 993–1001. [PubMed: 2467224]

Hilber B, Scholze P, Dorostkar MM, et al. (2005) Serotonin-transporter mediated efflux: a pharmacological analysis of amphetamines and non-amphetamines. Neuropharmacology 49(6): 811–819. [PubMed: 16185723]

Holmes A, Murphy DL and Crawley JN (2003a) Abnormal behavioral phenotypes of serotonin transporter knockout mice: parallels with human anxiety and depression. Biol Psychiatry 54(10): 953–959. [PubMed: 14625137]

Holmes A, Yang RJ, Lesch KP, et al. (2003b) Mice lacking the serotonin transporter exhibit 5-HT(1A) receptor-mediated abnormalities in tests for anxiety-like behavior. Neuropsychopharmacology 28(12): 2077–2088. [PubMed: 12968128]

Holmes A, Yang RJ, Murphy DL, et al. (2002) Evaluation of antidepressant-related behavioral responses in mice lacking the serotonin transporter. Neuropsychopharmacology 27(6): 914–923. [PubMed: 12464448]

Iversen L (2000) Neurotransmitter transporters: fruitful targets for CNS drug discovery. Mol Psychiatry 5(4): 357–362. [PubMed: 10889545]

Jennings KA, Loder MK, Sheward WJ, et al. (2006) Increased expression of the 5-HT transporter confers a low-anxiety phenotype linked to decreased 5-HT transmission. J Neurosci 26(35): 8955–8964. [PubMed: 16943551]

Kalueff AV, Fox MA, Gallagher PS, et al. (2007) Hypolocomotion, anxiety and serotonin syndrome-like behavior contribute to the complex phenotype of serotonin transporter knockout mice. Genes Brain Behav 6(4): 389–400. [PubMed: 16939636]

Kinsey SG, Bailey MT, Sheridan JF, et al. (2007) Repeated social defeat causes increased anxiety-like behavior and alters splenocyte function in C57BL/6 and CD-1 mice. Brain Behav Immun 21(4): 458–466. [PubMed: 17178210]

Kiyasova V, Fernandez SP, Laine J, et al. (2011) A genetically defined morphologically and functionally unique subset of 5-HT neurons in the mouse raphe nuclei. J Neurosci 31(8): 2756–2768. [PubMed: 21414898]

Koch S and Galloway MP (1997) MDMA induced dopamine release in vivo: role of endogenous serotonin. J Neural Transm (Vienna) 104(2–3): 135–146. [PubMed: 9203077]

Kulkarni SK, Singh K and Bishnoi M (2007) Elevated zero maze: a paradigm to evaluate antianxiety effects of drugs. Methods Find Exp Clin Pharmacol 29(5): 343–348. [PubMed: 17805436]

Liechti ME, Baumann C, Gamma A, et al. (2000) Acute psychological effects of 3,4-methylenedioxymethamphetamine (MDMA, "Ecstasy") are attenuated by the serotonin uptake inhibitor citalopram. Neuropsychopharmacology 22(5): 513–521. [PubMed: 10731626]

Line SJ, Barkus C, Coyle C, et al. (2011) Opposing alterations in anxiety and species-typical behaviours in serotonin transporter overexpressor and knockout mice. Eur Neuropsychopharmacol 21(1): 108–116. [PubMed: 20863670]

Lira A, Zhou M, Castanon N, et al. (2003) Altered depression-related behaviors and functional changes in the dorsal raphe nucleus of serotonin transporter-deficient mice. Biol Psychiatry 54(10): 960–971. [PubMed: 14625138]

Livak KJ and Schmittgen TD (2001) Analysis of relative gene expression data using real-time quantitative PCR and the 2(-Delta Delta C(T)) Method. Methods 25(4): 402–408. [PubMed: 11846609]

Martin-McCaffrey L, Hains MD, Pritchard GA, et al. (2005) Differential expression of regulator of G-protein signaling R12 subfamily members during mouse development. Dev Dyn 234(2): 438–444. [PubMed: 16145674]

Mayorga AJ and Lucki I (2001) Limitations on the use of the C57BL/6 mouse in the tail suspension test. Psychopharmacology (Berl) 155(1): 110–112. [PubMed: 11374330]

Meltzer HY (1990) Role of serotonin in depression. Ann N Y Acad Sci 600: 486–499; discussion 499–500. [PubMed: 2252328]

Mithoefer MC, Wagner MT, Mithoefer AT, et al. (2011) The safety and efficacy of {+/−}3,4-methylenedioxymethamphetamine-assisted psychotherapy in subjects with chronic, treatment-resistant posttraumatic stress disorder: the first randomized controlled pilot study. J Psychopharmacol 25(4): 439–452. [PubMed: 20643699]

Mosienko V, Bert B, Beis D, et al. (2012) Exaggerated aggression and decreased anxiety in mice deficient in brain serotonin. Transl Psychiatry 2: e122. [PubMed: 22832966]

Muzerelle A, Scotto-Lomassese S, Bernard JF, et al. (2016) Conditional anterograde tracing reveals distinct targeting of individual serotonin cell groups (B5-B9) to the forebrain and brainstem. Brain Struct Funct 221(1): 535–561. [PubMed: 25403254]

Nordquist N and Oreland L (2010) Serotonin, genetic variability, behaviour, and psychiatric disorders--a review. Ups J Med Sci 115(1): 2–10. [PubMed: 20187845]

Nutt DJ (2002) The neuropharmacology of serotonin and noradrenaline in depression. Int Clin Psychopharmacol 17 Suppl 1: S1–12.

Oehen P, Traber R, Widmer V, et al. (2013) A randomized, controlled pilot study of MDMA (+/−3,4-Methylenedioxymethamphetamine)-assisted psychotherapy for treatment of resistant, chronic Post-Traumatic Stress Disorder (PTSD). J Psychopharmacol 27(1): 40–52. [PubMed: 23118021]

Okaty BW, Commons KG and Dymecki SM (2019) Embracing diversity in the 5-HT neuronal system. Nat Rev Neurosci 20(7): 397–424. [PubMed: 30948838]

Oliver KH, Duvernay MT, Hamm HE, et al. (2016) Loss of Serotonin Transporter Function Alters ADP-mediated Glycoprotein alphaIIbbeta3 Activation through Dysregulation of the 5-HT2A Receptor. J Biol Chem 291(38): 20210–20219. [PubMed: 27422820]

Owens MJ and Nemeroff CB (1994) Role of serotonin in the pathophysiology of depression: focus on the serotonin transporter. Clin Chem 40(2): 288–295. [PubMed: 7508830]

Parrott AC (2002) Recreational Ecstasy/MDMA, the serotonin syndrome, and serotonergic neurotoxicity. Pharmacol Biochem Behav 71(4): 837–844. [PubMed: 11888574]

Parrott AC (2004) Is ecstasy MDMA? A review of the proportion of ecstasy tablets containing MDMA, their dosage levels, and the changing perceptions of purity. Psychopharmacology (Berl) 173(3–4): 234–241. [PubMed: 15007594]

Pratt LA, Brody DJ and Gu Q (2017) Antidepressant Use Among Persons Aged 12 and Over:United States,2011–2014. NCHS Data Brief Epub ahead of print 2017/11/21.(283): 1–8.

Rothman RB and Baumann MH (2003) Monoamine transporters and psychostimulant drugs. Eur J Pharmacol 479(1–3): 23–40. [PubMed: 14612135]

Rothman RB, Baumann MH, Dersch CM, et al. (2001) Amphetamine-type central nervous system stimulants release norepinephrine more potently than they release dopamine and serotonin. Synapse 39(1): 32–41. [PubMed: 11071707]

Rudnick G and Wall SC (1992) The molecular mechanism of "ecstasy" [3,4-methylenedioxy-methamphetamine (MDMA)]: serotonin transporters are targets for MDMA-induced serotonin release. Proc Natl Acad Sci U S A 89(5): 1817–1821. [PubMed: 1347426]

Sandtner W, Stockner T, Hasenhuetl PS, et al. (2016) Binding Mode Selection Determines the Action of Ecstasy Homologs at Monoamine Transporters. Mol Pharmacol 89(1): 165–175. [PubMed: 26519222]

Schindler AG, Messinger DI, Smith JS, et al. (2012) Stress produces aversion and potentiates cocaine reward by releasing endogenous dynorphins in the ventral striatum to locally stimulate serotonin reuptake. J Neurosci 32(49): 17582–17596. [PubMed: 23223282]

Shepherd JK, Grewal SS, Fletcher A, et al. (1994) Behavioural and pharmacological characterisation of the elevated "zero-maze" as an animal model of anxiety. Psychopharmacology (Berl) 116(1): 56–64. [PubMed: 7862931]

Sialana FJ, Wang AL, Fazari B, et al. (2018) Quantitative Proteomics of Synaptosomal Fractions in a Rat Overexpressing Human DISC1 Gene Indicates Profound Synaptic Dysregulation in the Dorsal Striatum. Front Mol Neurosci 11: 26. [PubMed: 29467617]

Snow BE, Antonio L, Suggs S, et al. (1997) Molecular cloning and expression analysis of rat Rgs12 and Rgs14. Biochem Biophys Res Commun 233(3): 770–777. [PubMed: 9168931]

Snow BE, Hall RA, Krumins AM, et al. (1998) GTPase activating specificity of RGS12 and binding specificity of an alternatively spliced PDZ (PSD-95/Dlg/ZO-1) domain. J Biol Chem 273(28): 17749–17755. [PubMed: 9651375]

Soundararajan M, Willard FS, Kimple AJ, et al. (2008) Structural diversity in the RGS domain and its interaction with heterotrimeric G protein alpha-subunits. Proc Natl Acad Sci U S A 105(17): 6457–6462. [PubMed: 18434541]

Spanos LJ and Yamamoto BK (1989) Acute and subchronic effects of methylenedioxymethamphetamine [(+/−)MDMA] on locomotion and serotonin syndrome behavior in the rat. Pharmacol Biochem Behav 32(4): 835–840. [PubMed: 2572003]

Steru L, Chermat R, Thierry B, et al. (1985) The tail suspension test: a new method for screening antidepressants in mice. Psychopharmacology (Berl) 85(3): 367–370. [PubMed: 3923523]

Sundaramurthy S, Annamalai B, Samuvel DJ, et al. (2017) Modulation of serotonin transporter function by kappa-opioid receptor ligands. Neuropharmacology 113(Pt A): 281–292. [PubMed: 27743931]

Suri D, Teixeira CM, Cagliostro MK, et al. (2015) Monoamine-sensitive developmental periods impacting adult emotional and cognitive behaviors. Neuropsychopharmacology 40(1): 88–112. [PubMed: 25178408]

Teissier A, Chemiakine A, Inbar B, et al. (2015) Activity of Raphe Serotonergic Neurons Controls Emotional Behaviors. Cell Rep 13(9): 1965–1976. [PubMed: 26655908]

Uhl GR and Johnson PS (1994) Neurotransmitter transporters: three important gene families for neuronal function. J Exp Biol 196: 229–236. [PubMed: 7823024]

Walf AA and Frye CA (2007) The use of the elevated plus maze as an assay of anxiety-related behavior in rodents. Nat Protoc 2(2): 322–328. [PubMed: 17406592]

Willard MD, Willard FS, Li X, et al. (2007) Selective role for RGS12 as a Ras/Raf/MEK scaffold in nerve growth factor-mediated differentiation. EMBO J 26(8): 2029–2040. [PubMed: 17380122]

Yadav PN, Abbas AI, Farrell MS, et al. (2011) The presynaptic component of the serotonergic system is required for clozapine's efficacy. Neuropsychopharmacology 36(3): 638–651. [PubMed: 21048700]

Ye R, Carneiro AM, Airey D, et al. (2014) Evaluation of heritable determinants of blood and brain serotonin homeostasis using recombinant inbred mice. Genes Brain Behav 13(3): 247–260. [PubMed: 24102824]

Ye R, Quinlan MA, Iwamoto H, et al. (2015) Physical Interactions and Functional Relationships of Neuroligin 2 and Midbrain Serotonin Transporters. Front Synaptic Neurosci 7: 20. [PubMed: 26793096]

Yu Q, Teixeira CM, Mahadevia D, et al. (2014) Dopamine and serotonin signaling during two sensitive developmental periods differentially impact adult aggressive and affective behaviors in mice. Mol Psychiatry 19(6): 688–698. [PubMed: 24589889]

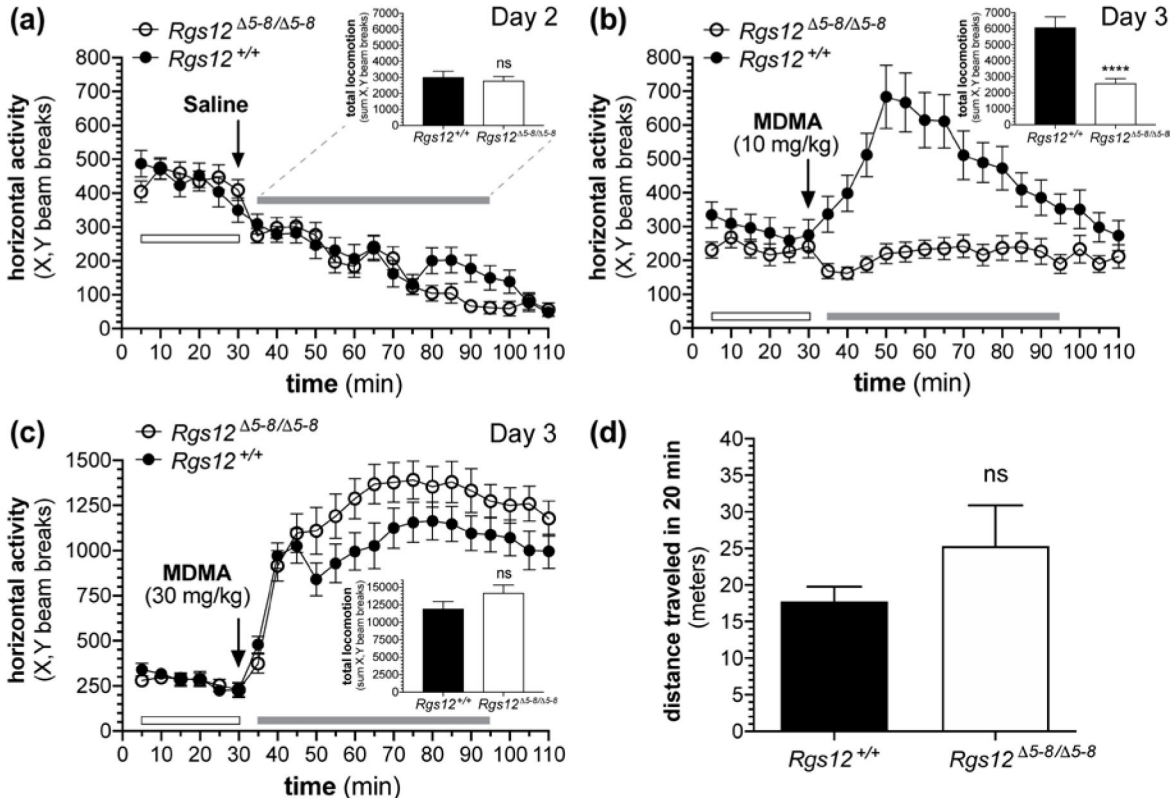

Figure 1.

MDMA-induced locomotor activity in RGS12-null mice. (**a**) Baseline (first 30 min; open bar) and control injection (saline)-induced locomotion by RGS12-null (*Rgs12*$^{\Delta 5-8/\Delta 5-8}$) mice and wild-type (*Rgs12*$^{+/+}$) littermate controls. *Inset*, Bar graph of cumulative locomotion over 60 min post-saline injection (grey bar), derived from data in panel **a**. (**b**) Baseline (first 30 min) and 10 mg/kg MDMA-induced locomotion by RGS12-null (*Rgs12*$^{\Delta 5-8/\Delta 5-8}$) mice and wild-type (*Rgs12*$^{+/+}$) littermate controls. *Inset*, Cumulative locomotion over 60 min post-MDMA injection, derived from data in panel **b**. (**c**) Baseline and 30 mg/kg MDMA-induced hyperlocomotion in RGS12-null mice and wild-type littermates. *Inset*, Cumulative locomotion over 60 min post-MDMA injection, derived from data in panel **c**. All data are presented as the mean ± SEM (*n* = 22–23 mice per group) and were analyzed by two-way ANOVA or, for cumulative locomotion bar-graph insets, by Student's *t*-test or Mann-Whitney U test (see Results for more details). (**d**) Spontaneous home-cage locomotor activity by RGS12-null (*Rgs12*$^{\Delta 5-8/\Delta 5-8}$) mice and wild-type (*Rgs12*$^{+/+}$) littermate controls (mean ± SEM; n = 3 mice per genotype).

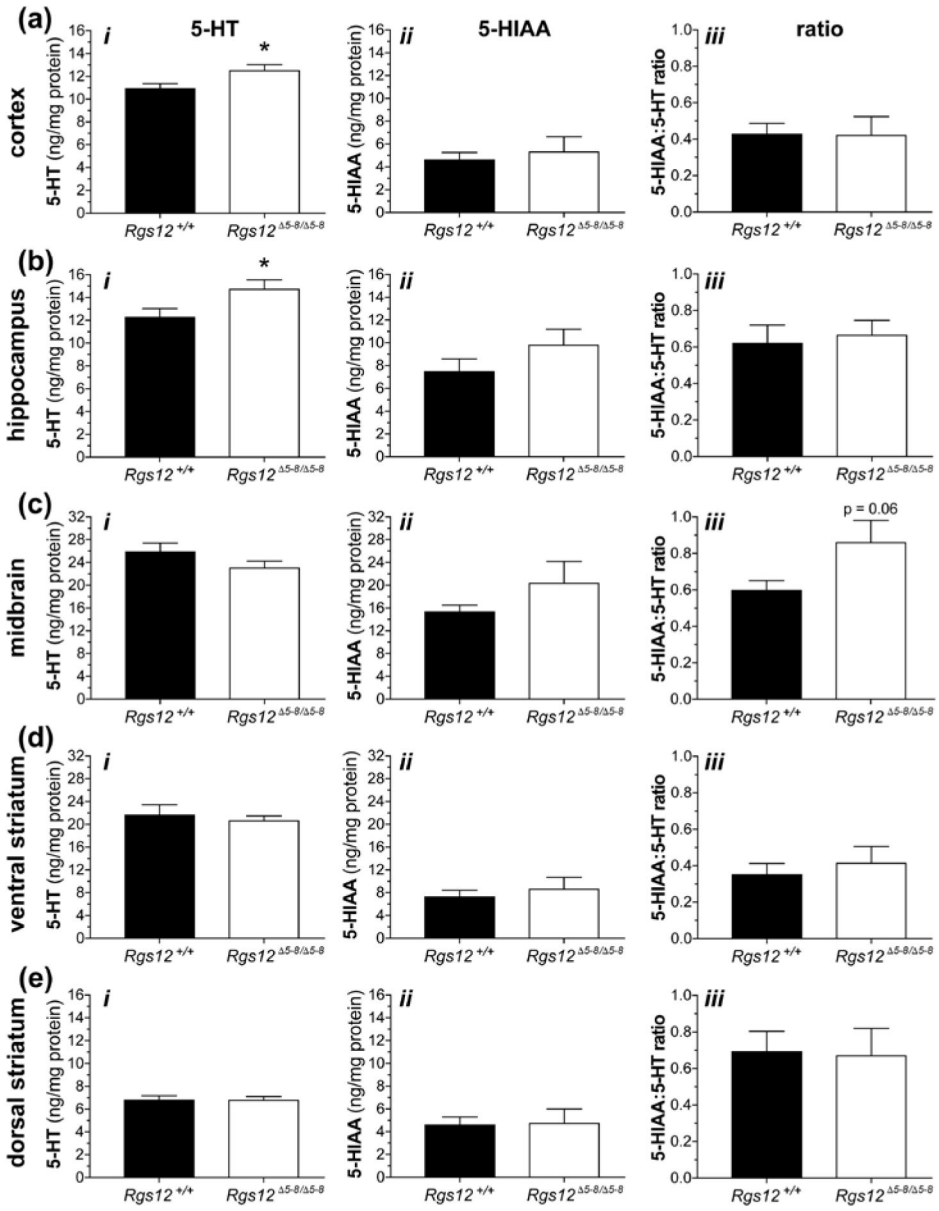

Figure 2.

Measurement of baseline tissue levels of 5-HT (***i***), its major metabolite 5-HIAA (***ii***), and their computed ratio (***iii***) in selected brain regions of RGS12-null and wild-type mice, including cortex **(a)**, hippocampus **(b)**, midbrain **(c)**, ventral striatum **(d)**, and dorsal striatum **(e)**. Data are presented as the mean ± SEM (n = 6 mice per group) and were analyzed by Student's t-test. *, $p < 0.05$.

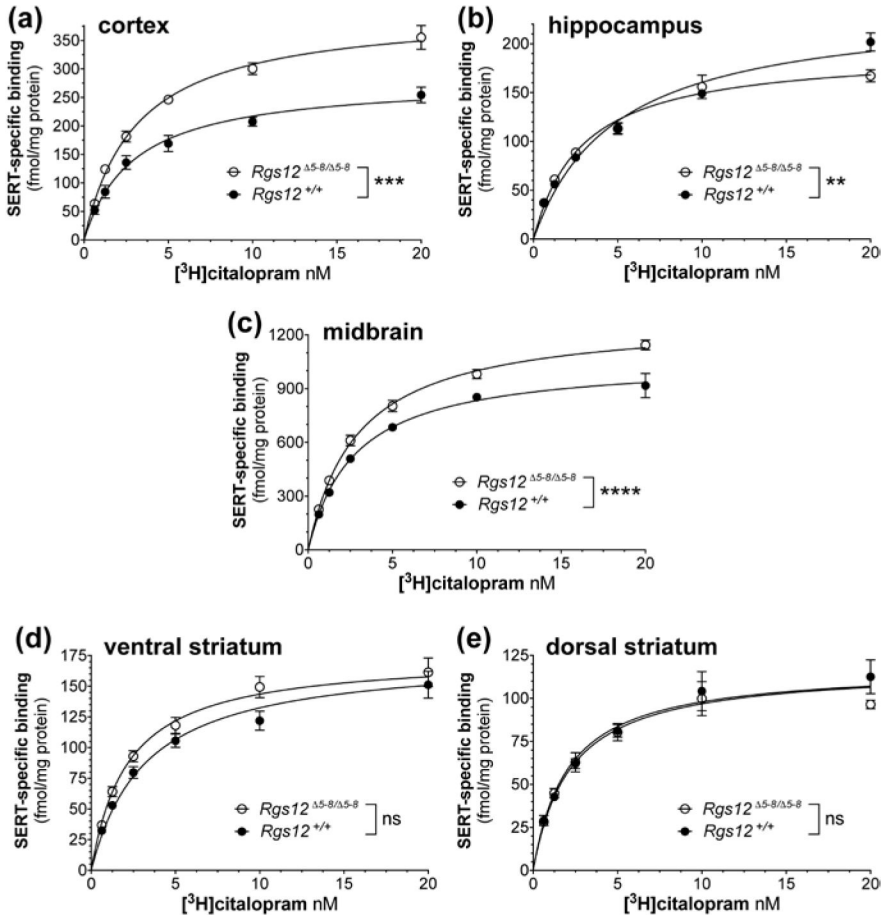

Figure 3.

Analysis of SERT expression/binding sites by radioligand saturation binding. [^{3}H]citalopram binding to SERT in membrane preparations from **(a)** cortex, **(b)** hippocampus, **(c)** midbrain, **(d)** ventral striatum, and **(e)** dorsal striatum of RGS12-null mice and wild-type littermate controls. Non-specific binding was determined in the presence of 10 μM cold citalopram. Data are presented as the mean ± SEM (n = 6–15 mice per group) and were analyzed by nonlinear regression. Asterisks denote a statistically significant difference in the number of SERT binding sites (B_{max}) between genotypes. Significance derived from F-tests of curve fits: ns, not significant ($p > 0.05$); **, $p < 0.01$; ***, $p < 0.001$; **** $p < 0.0001$. The affinity of [^{3}H]citalopram for SERT (K_d) differed between genotypes in the hippocampus, but not in any other brain region tested ($p > 0.05$).

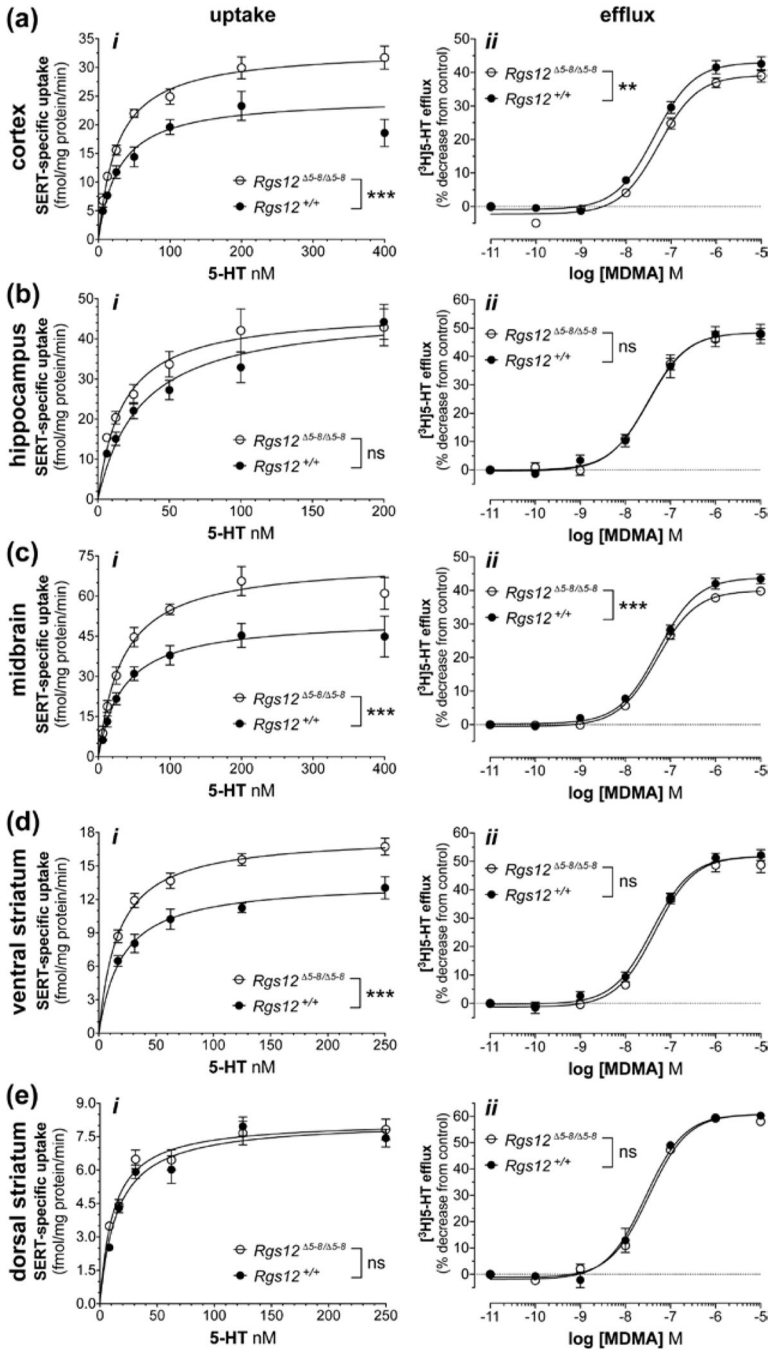

Figure 4.

Assessment of SERT-specific [^{3}H]5-HT uptake and MDMA-stimulated [^{3}H]5-HT efflux in synaptosomal preparations from indicated brain regions of RGS12-null and wild-type mice. SERT-specific [^{3}H]5-HT uptake (***i*** panels) in synaptosomal preparations from **(a)** cortex, **(b)** hippocampus, **(c)** midbrain, **(d)** ventral striatum, and **(e)** dorsal striatum. Data are presented as the mean ± SEM (n = 6–12 mice per group) and were analyzed by nonlinear regression to derive values for V_{max} and K_m. Asterisks denote a statistically significant difference of maximal uptake rates (V_{max}) between genotypes; significance derived from F-tests of curve

fits: ns, not significant ($p > 0.05$); ***, $p < 0.001$. No differences in the affinity (K_m) of [^{3}H]5-HT for SERT were identified for any brain regions tested ($p > 0.05$). Analyses of SERT-specific MDMA-stimulated [^{3}H]5-HT efflux (***ii*** panels) in preloaded synaptosomal preparations from **(a)** cortex, **(b)** hippocampus, **(c)** midbrain, **(d)** ventral striatum, and **(e)** dorsal striatum of RGS12-null mice and wild-type littermate controls. Data are the mean ± SEM (n = 6–15 mice per group) and were analyzed by nonlinear regression. Asterisks denote a statistically significant difference of efficacy (E_{max}) between genotypes; significance derived from F-tests of curve fits: **, $p < 0.01$; ***, $p < 0.001$. No differences in MDMA efflux potency (pEC_{50}) were observed for any brain regions tested.

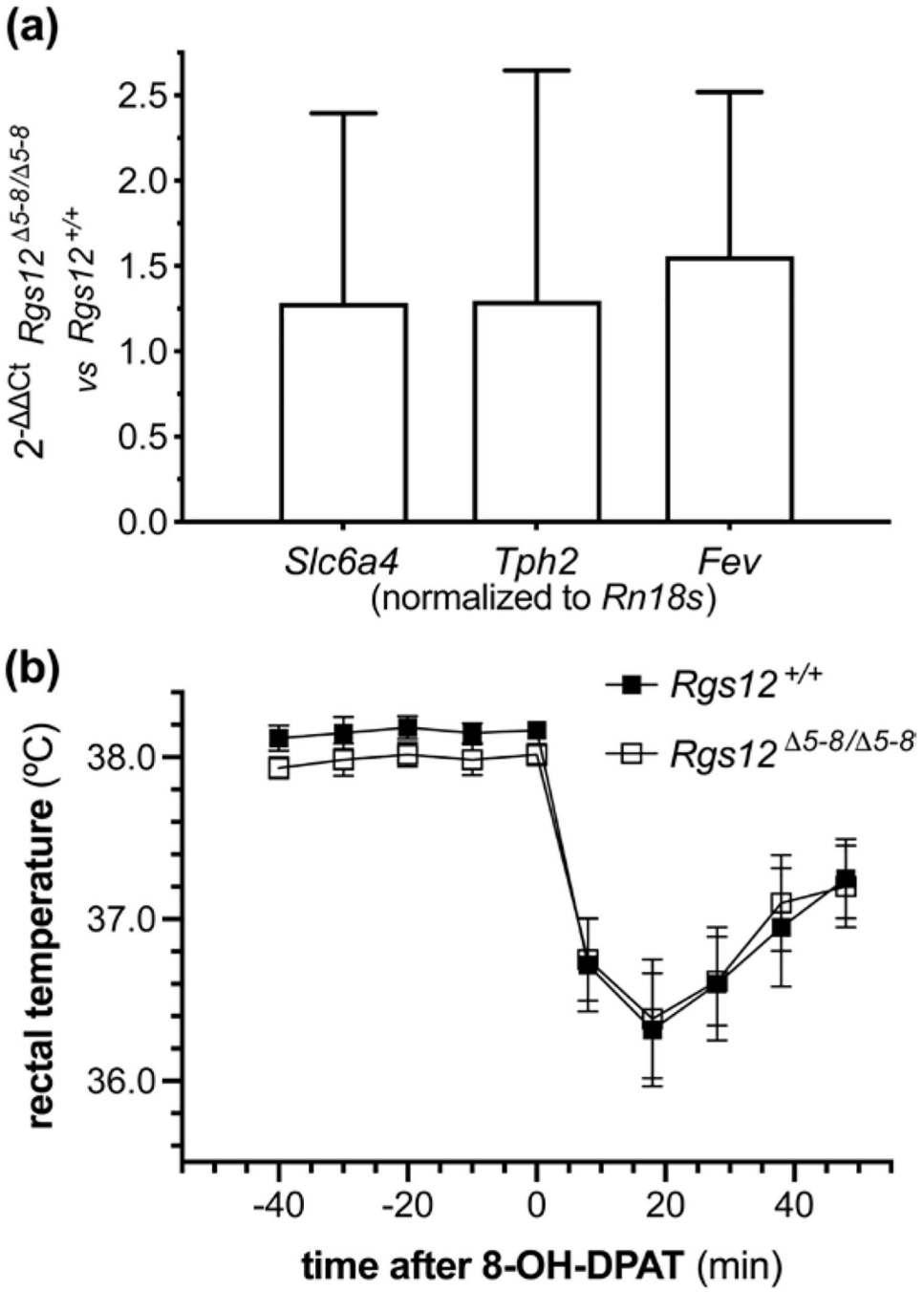

Figure 5.

Analyses of brain region relative mRNA expression and 5-HT_{1A} receptor agonist-induced hypothermia in RGS12-null mice. (**a**) Relative mRNA expression levels of *Slc6a4* (encoding SERT), *Tph2* (encoding tryptophan hydroxylase 2), and *Fev* (encoding the serotonergic neuron marker/transcription factor Pet-1) are unaltered in *Rgs12*-null mice. Data are reported as the mean ± SEM (n = 3 mice/genotype). (**b**) Hypothermia induced by 8-OH-DPAT (0.5 mg/kg, ip) is unaltered in RGS12-null mice. Data are reported as the mean ± SEM (n = 6 mice/genotype).

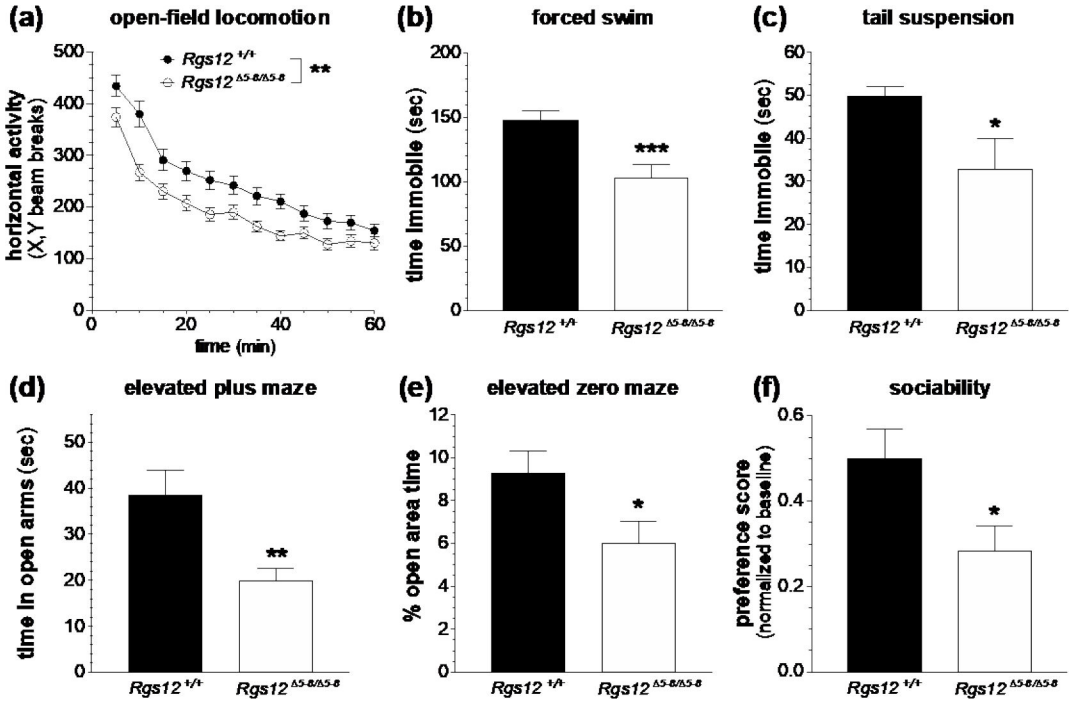

Figure 6.

Evaluation of serotonergically modulated behaviors in RGS12-null mice. **(a)** Open-field locomotor activity over 60 min in naïve RGS12-null mice and wild-type littermate controls upon their first exposure to the activity chambers. Data are presented as the mean ± SEM of $n = 76–79$ mice per group. **(b)** Immobility time in the forced swim test exhibited by RGS12-null mice and wild-type littermate controls. Data are presented as the mean ± SEM ($n = 18–23$ mice per group) and were analyzed by Student's t-test (***, $p < 0.001$). **(c)** Immobility time in the tail suspension test displayed by RGS12-null mice and wild-type littermate controls. Data are presented as the mean ± SEM ($n = 7–8$ mice per group) and were analyzed by Student's t-test (*, $p < 0.05$). **(d)** Time spent in the open arms of the elevated plus maze by RGS12-null mice and wild-type littermate controls. Data are presented as the mean ± SEM ($n = 11–13$ mice per group) and were analyzed by Student's t-test (**, $p < 0.01$). **(e)** Percentage of time spent in the open areas of the elevated zero maze by RGS12-null mice and wild-type littermate controls. Data are presented as the mean ± SEM ($n = 17–18$ mice per group) and were analyzed by Student's t-test (***, $p < 0.001$). **(f)** Test of sociability by RGS12-null mice and wild-type littermate controls. Data are presented as the mean ± SEM ($n = 17–24$ mice per group) and were analyzed by Student's t-test (*, $p < 0.05$).

Table 1.

Summary of values derived from *ex vivo* biochemical determinations of SERT binding sites and synaptosomal serotonin uptake and efflux in indicated brain regions of RGS12-null mice and wild-type littermate controls.

	Rgs12$^{+/+}$		*Rgs12*$^{\Delta 5-8/\Delta 5-8}$	
	[^{3}H]citalopram binding			
	B_{max} (fmol/mg)	K_d (nM)	B_{max} (fmol/mg)	K_d (nM)
cortex	281. 5 ± 14.3	2.9 ± 0.4	402.9 ± 13.6	3.0 ± 0.3
hippocampus	238. 9 ± 11.6	4.8 ± 0.6	192.7 ± 8.0	2.9 ± 0.3
midbrain	1063 ± 36.8	2.7 ± 0.2	1294 ± 33.7	2.9 ± 0.2
ventral striatum	165.3 ± 7.8	2.7 ± 0.4	181.4 ± 7.9	2.4 ± 0.3
dorsal striatum	126.8 ± 7.3	2.4 ± 0.4	110.2 ± 5.3	1.8 ± 0.3
	[^{3}H]5-HT uptake			
	V_{max} (fmol/mg/min)	K_m (nM)	V_{max} (fmol/mg/min)	K_m (nM)
cortex	24.7 ± 1.7	28.6 ± 6.5	33.2 ± 1.2	26.9 ± 3.4
hippocampus	46.7 ± 3.8	29.7 ± 7.0	47.2 ± 3.6	17.6 ± 5.1
midbrain	51.4 ± 3.6	34.7 ± 8.0	73.1 ± 3.9	33.9 ± 6.0
ventral striatum	13.6 ± 0.7	20.2 ± 4.6	17.7 ± 0.6	16.7 ± 2.5
dorsal striatum	8.2 ± 0.4	15.3 ± 3.5	8.1 ± 0.3	11.6 ± 2.4
	MDMA-elicited [^{3}H]5-HT efflux			
	E_{max} (maximal % decrease *vs* vehicle control)	pEC_{50}	E_{max} (maximal % decrease *vs* vehicle control)	pEC_{50}
cortex	43.0 ± 1.0	7.3 ± 0.06	39.1 ± 0.9	7.2 ± 0.06
hippocampus	48.7 ± 1.7	7.4 ± 0.1	48.0 ± 1 .2	7.5 ± 0.07
midbrain	43.8 ± 0.8	7.2 ± 0.05	39.9 ± 0.6	7.2 ± 0.04
ventral striatum	52.9 ± 1.1	7.3 ± 0.06	50.1 ± 1 .2	7.3 ± 0.06
dorsal striatum	61.3 ± 1.4	7.5 ± 0.06	60.2 ± 0.8	7.4 ± 0.04

Data from at least three experiments were fit to the appropriate mathematical model using Prism 8 to determine the best-fit values (± SE) for the indicated measures.